Optical Probes of Excited States in Poly(*p*-Phenylenevinylene)

J. M. Leng, S. Jeglinski, X. Wei, R. E. Benner, and Z. V. Vardeny
Department of Physics and Electrical Engineering, University of Utah, Salt Lake City, Utah 84112

F. Guo and S. Mazumdar
Physics Department, University of Arizona, Tucson, Arizona 85721
(Received 1 September 1993)

We have studied electronic excited states in films of poly(*p*-phenylenevinylene) using picosecond transient and cw photomodulation, photoluminescence, and their excitation spectra, as well as electroabsorption spectroscopy. We have determined all the important energy levels of singlet excitons with odd and even parity, the onset of the continuum band, the two-electron (biexciton) states, and the two relevant triplet states, and show that good agreement exists with models involving electron correlation.

PACS numbers: 78.47.+p, 72.20.Jv, 78.55.Kz, 78.66.Qn

The photophysics and resonant nonlinear optical properties of conducting polymers are dominated by the locations and natures of the excited-state energy levels. These excited states include singlet excitons with odd (B_u) and even (A_g) parity, the continuum band (CB), two-electron (biexciton) states, and the triplet manifold [1,2]. Recent theoretical advances in the area of subgap third-order optical nonlinearity [3,4] provide information about a subset of the excited states, which include the lowest B_u exciton ($1B_u$), a dominant A_g exciton (hereafter the mA_g), and the CB threshold. The relative locations of the $1B_u$ and the lowest A_g ($2A_g$) excitons are determined by a sensitive interplay between electron-electron interaction and alternation (δ) in the π electron transfer integral along the polymer chain [5]. For realistic Coulomb interaction and small δ [5], the optical gap E_g to the $1B_u$ exciton is relatively small, the $2A_g$ lies below the $1B_u$, and, due to the dipole forbidden character of the lowest singlet, photoluminescence (PL) is weak. Large δ results in larger E_g, state ordering $E(2A_g) > E(1B_u)$, and consequently high PL efficiency with promising applications in displays [such as light emitting diodes (LED) [6]]. The benzene ring in the backbone structure of poly(*p*-phenylenevinylene) (PPV) yields an effective δ for the extended π states that is large [2], and therefore PPV belongs to the latter category. Nevertheless, Coulomb interaction among the π electrons in PPV leads to behavior qualitatively different from the predictions of single-particle Hückel or SSH models.

Recent subpicosecond PL [7] and site-selection PL [8] have demonstrated that the primary excitation in PPV is to an exciton, and that the associated lattice relaxation energy is small. This already suggests a subsidiary role of the electron-phonon interaction. The location of the mA_g exciton has been determined by two-photon luminescence [9], whereas long-lived triplet excitons have been found in thin films [10,11] and LEDs [12]. In the present work, we present a more complete picture of the various photoexcitations and excited states in PPV, based on a variety of optical probes including picosecond transient and cw photomodulation (PM) and PL and their excitation dependence, and the electroabsorption (EA) technique. We have tentatively mapped the most relevant singlet and triplet electronic manifolds, including the CB threshold and the lowest biexciton, that are not seen in direct optical absorption. Agreement with model calculations within Coulomb correlated models strengthens our assignments.

The spectral evolution of the excited states in the picosecond time domain was studied by the pump and probe PM transient technique using two dye lasers synchronously pumped by a frequency-doubled mode-locked Nd:YAG laser at a repetition rate of 76 MHz with 5 ps resolution, and by a streak camera with 10 ps resolution of the PL transient. Transient spectra of photoinduced changes ΔT in transmission T were obtained by fixing the pump wavelength at 570 nm (2.17 eV) and varying the probe wavelength between 1.2 and 2.2 eV. For the cw PM measurements the excitation was an Ar^+ laser beam modulated at frequency f between 20 Hz and 1 MHz by an acousto-optic modulator, and the probe beam source was a premonochromatized tungsten lamp. $\Delta T(f)$ was measured by a set of fast detectors with matched preamplifiers and a lock-in amplifier. For the excitation dependencies of the PL and various bands in the PM spectrum we used a premonochromatized 300 W xenon lamp modulated at 150 Hz. The excitation intensity was normalized by the absorption, reflection, and the detection setup to yield a quantum-efficiency spectrum per absorbed photon.

The PPV sample was a film polymerized on a sapphire substrate with thickness of about 30 μm. The EA spectrum was measured on a thin (< 500 Å) PPV-MEH film spun cast directly on a pair of interlocked electrodes with gaps of 20 μm capable of supporting modulated fields up to 10^6 V/cm; the EA signal was measured at $2f$ where f (500 Hz) is the field modulation.

The transient PM spectrum at 300 K obtained with the synchronously pumped system at $t=0$ is shown in Fig. 1. We observed a broad photoinduced absorption (PA) band (labeled EX), which differs substantially from the cw PA bands (also shown in Fig. 1). The EX band peaks at 1.75

0031-9007/93/72(1)/156(4)$06.00

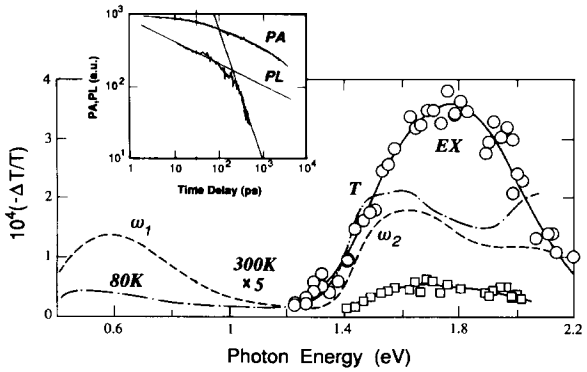

FIG. 1. PM spectra of PPV in the picosecond time domain (open circles for $t=0$, open squares for $t=1$ ns) and cw at 80 K (dot-dashed line) and 300 K (broken line). The full lines through the picosecond data points are guides to the eye. Various PA bands (EX, T, ω_1, and ω_2) are assigned. The inset shows the PA (at 1.7 eV) and PL decays and their asymptotic fits (see text).

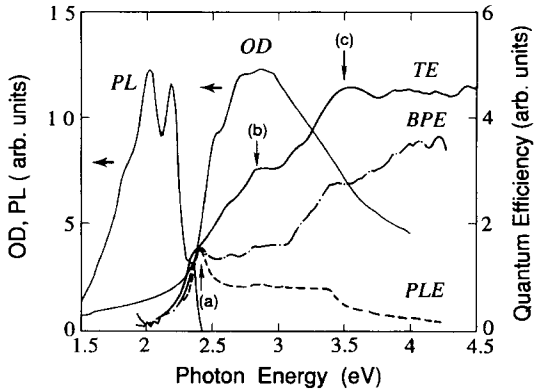

FIG. 2. PPV excitation spectra of PL (PLE), $BP^{2\mp}$ (BPE), and triplets (TE). The PL band and an OD spectrum are also shown. Bands a, b, and c are assigned (see text).

eV and remains essentially unchanged up to 3 ns. For example, the PA spectrum at 1 ns (open squares) is compared to that at $t=0$ (open circles) in Fig. 1. The small redshift of the PA peak at longer times to about 1.7 eV is too tiny to account for a possible drastic change in the photoexcitation properties. We conclude that the dominant photoexcitations at 3 ns are the same as those generated at $t=0$.

The dynamics of the EX band from 10 ps to 3 ns are shown in Fig. 1 (inset) for a probe photon energy of 1.4 eV; the dynamics were the same for all probe wavelengths. We have also checked that the dynamics do not change with increasing excitation density from 10^{17} to 10^{18} cm^{-3}, thus excluding bimolecular kinetics. The PA decay is very well fit by a formula based on monomolecular recombination caused by dispersive trapping in amorphous semiconductors [13]

$$n(t)=\frac{n(0)}{1+(t/\tau)^{\beta}}, \qquad (1)$$

where $n(t)$ is the photoexcitation density $[-\Delta T/T\approx n(t)]$, τ (=215 ps) is the trapping or recombination time, and β (=0.65) is the dispersion parameter characterizing the dispersive relaxation. This implies that the photoexcitations in the picosecond time domain recombine at recombination centers and their diffusion towards these centers is time dependent because of shallow traps. This is consistent with the slight PA redshift with time in the EX band observed in Fig. 1 and in the spectrally resolved transient PL [7]; this may be due to migration and thermalization of excitons within the inhomogeneous chain distribution [14].

The t_{PL} decay from 10 to 400 ps is also shown in Fig. 1 (inset). It is much faster than t_{PA} and is well fit by two power law asymptotes: For $t\ll\tau$, $t_{PL}\sim t^{-\gamma_1}$, whereas $t_{PL}\sim t^{-\gamma_2}$ for $t\gg\tau$. These are actually asymptotes of the t_{PA} derivative given by Eq. (1) [15]. Remarkably, we obtained for the exponents $\gamma_1+\gamma_2\simeq 2$ and thus they can be deduced from one parameter β_0 with $\gamma_1=1-\beta_0$ and $\gamma_2=1+\beta_0$ with $\beta_0=0.75$, close to the parameter β (=0.65) deduced from t_{PA}. Moreover, the intercept of the two asymptotic fits to t_{PL} occurs at 210 ps, very close to τ (=215 ps) deduced from t_{PA}. From the asymptotic behavior of t_{PA} and t_{PL} (Fig. 1) we conclude that they are related since $t_{PA}\sim n(t)$ whereas $t_{PL}\sim dn/dt$. Consequently, the dominant photoexcitations in the ps to ns time ranges are *excitons*, consistent with the fs PL measurements [7]. The relation $t_{PL}=dt_{PA}/dt$ implies that nonradiative decay channels are negligibly small for $t<400$ ps; beyond 400 ps we indeed found that t_{PL} substantially deviates from dt_{PA}/dt.

The cw PM spectra at 80 and 300 K are also shown in Fig. 1. The PA band T at 1.45 eV which dominates the PM spectrum at 80 K is due to triplets [10,11], whereas the two correlated PA bands ω_1 at 0.55 eV and ω_2 at 1.6 eV, respectively, which dominate the PM spectrum at 300 K are due to charged bipolarons ($BP^{2\mp}$) [10,11]. In contrast, the EX band in the picosecond time domain (Fig. 1) is quite different from all cw PA bands, consistent with its different assignment associated with photoexcited B_u excitons. That EX is not arising from separated charged polarons can be inferred also from the geminate recombination nature of t_{PA} in the nanosecond time domain. This was confirmed by measuring the PA decay upon decreasing the photoexcitation density by a factor of 10: The PA signal at short time depends linearly on the excitation intensity I_L and its relaxation kinetics remains unchanged with I_L.

Figure 2 shows the normalized excitation spectra of the cw PL (PLE), triplet (TE), and BP (BPE) PA bands in the cw PM spectrum measured at 2.2, 1.45, and 0.55 eV, respectively, together with the PL spectrum and a typical optical density (OD) of PPV. All three excitation spectra show a peak at 2.4 eV (a in Fig. 2), close to a prominent shoulder in the OD. Since this peak is very close to the

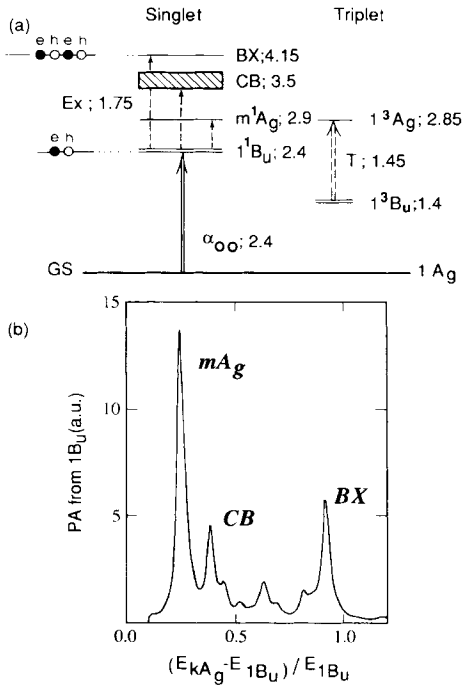

FIG. 3. (a) Excited state energy levels of PPV and the optical transitions from the 1^1B_u and 1^3B_u states. CB is the continuum band threshold and BX is the two-electron (biexciton) state (its *e-h* structure is shown). The allowed optical transitions are between states of opposite parity and *e-h* symmetry. (b) Calculated PA from the photogenerated 1^1B_u exciton (see text); the probe photon energy is given with respect to $E(1B_u)$, in units of $E(1B_u)$.

0-0 transition in the PL spectrum (Fig. 2), we identify it as the level of the $1B_u$ exciton in PPV; this is shown in the energy level diagram of Fig. 3(a). The appearance of the $1B_u$ exciton in all of the excitation spectra in Fig. 2 proves its important role in the photophysics of PPV. This is consistent with our picosecond results showing that the $1B_u$ excitons are the primary excitations in PPV. Their subsequent dissociation at defects, impurities, and interfaces leads to charge separation, whereas intersystem crossing leads to triplet generation.

The TE spectrum is very different from either the BPE or the PLE spectra up to about 3 eV (Fig. 2). This indicates that triplet generation channels different from the singlet-triplet intersystem crossing, which peaks at the 1^1B_u level, open up at high excitation energies. It is known that there exist covalent ^1A_g states (in particular the $2A_g$) above the 1^1B_u. These covalent states can be reached either by internal conversion from higher vibrational levels of the 1^1B_u or from the decay of higher B_u excitons (for, e.g., the 2^1B_u). As discussed by Tavan and Schulten [16], covalent singlet excitations are combinations of triplet excitations, in the limit of zero bond alternation. For large bond alternation, the ^1A_g states have lower energy than two triplets, but the difference in energy is small. Thus it is entirely conceivable that high vibrational levels of the covalent A_g states have sufficient

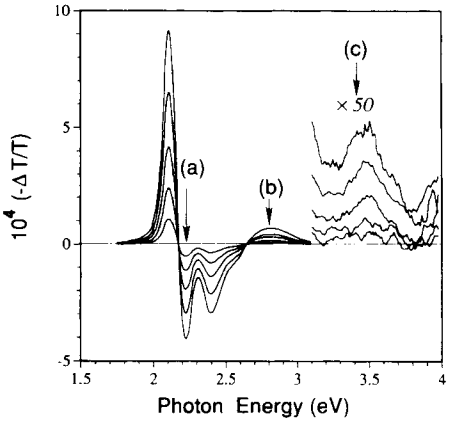

FIG. 4. Electroabsorption spectra of PPV-MEH at 80 K at various electric fields ranging from 2×10^5 to 6×10^5 V/cm. *a*, *b*, and *c* spectral features are assigned (see text).

energy for singlet fission, leading to triplets [17]. We believe that such singlet fission accounts for the new channels. We speculate that the plateau at 2.8 eV corresponds to exactly twice the energy of the 1^3B_u, which then is at 1.4 eV. The strong transition in the triple manifold is from the 1^3B_u, which is covalent, to ionic ^3A_g state. The lowest ionic ^1A_g state is the mA_g [1], and finite chain calculations suggest that the lowest ionic even parity states in the singlet and triplet manifolds are very close in energy for large bond alternation. This together with the recent determination of the mA_g at 2.95 eV [9] supports the above assignment.

The TE spectrum reaches its maximum at 3.5 eV, which we assign to the CB threshold. It has recently been demonstrated [18] that the CB in conjugated polymers consists of closely spaced delocalized A_g and B_u levels, and inside the CB the triplet states are also degenerate. Intersystem crossing thus becomes most efficient within the CB. Further support for this assignment comes from the BPE and PLE spectra, which show prominent features at 3.5 eV. It is obvious that once the CB is reached, the quantum efficiency for charge separation leading to long lived BP is expected to increase dramatically, whereas the opposite is true for the PL efficiency, which sharply decreases at CB (Fig. 2).

The above assignments are also supported by our EA measurements. In principle, the m^1A_g state can be detected in EA spectroscopy, since the strong applied electric field in EA mixes B_u and A_g states, and consequently gives oscillator strength to the otherwise forbidden mA_g [18]. Figure 4 shows the EA spectrum of a PPV-MEH film [19]. It contains two prominent spectral features (*a* and *b* in Fig. 4): a derivativelike feature at 2.15 eV (followed by phonon sidebands) and a peak at 2.8 eV, respectively. In addition, a much weaker oscillatory feature at 3.5 eV can be observed (*c* in Fig. 4). Since the 2.15 eV feature can be reproduced by absorption derivatives, whereas the 2.8 eV peak cannot, we identify the former as caused by a Stark shift of the $1B_u$ exci-

ton in PPV-MEH [20] and the latter as caused by the mA_g state [19]. In contrast to the mA_g peak, the feature at 3.5 eV in EA is oscillatory in nature indicating that this is the CB threshold in PPV [18,21]. We note that the CB contribution in EA is weakened in disordered polymer films such as ours [22]. The CB threshold at 3.5 eV gives a binding energy $E_b = 1.1$ eV for the $1B_u$ exciton. This large E_b identifies the $1B_u$ exciton properties in PPV as charge-transfer type and casts doubt on the recently calculated $E_b = 0.4$ eV based on a model involving Wannier type excitons [23].

The threshold for the two-electron states (biexciton) (BX) where two e-h pairs are bound together [Fig. 3(a)] must be much lower than $2E(1B_u)$ (=4.8 eV), since extra Coulomb attractions exist between the electron and hole on the two adjacent excitons [24]. On the other hand, $E(\mathrm{BX}) > 2E(1B_u) - E_b = 3.7$ eV since there also exist in BX excess Coulomb repulsion (e-e and h-h). We therefore place $E(\mathrm{BX})$ in PPV to be between 3.7 and 4.8 eV. This determines the optical transition $1B_u \rightarrow \mathrm{BX}$ [Fig. 3(a)] to between 1.3 and 2.4 eV. We identify the PA band EX in Fig. 1, which is associated with photoexcited $1B_u$, as the transition into a BX state. EX peaks at 1.75 eV and this places the BX state in Fig. 3(a) at 4.15 eV. The BX binding energy (=0.65 eV) is therefore substantial in PPV.

The above assignment of the EX band to biexcitons is supported by our model approximate calculation within an extended Hubbard Hamiltonian [18] with an on-site Coulomb repulsion $U = 3t$, nearest neighbor interaction $V = t$, and $\delta = 0.2t$ for a 16 site linear chain. Here t is the nearest neighbor hopping integral. Our purpose is merely to demonstrate that substantial optical transitions can occur from the 1^1B_u states to excited ^1A_g states including the mA_g, CB threshold, and a state that is slightly below $2E(1^1B_u)$; an energy region that has not been previously probed theoretically. Energies of highly excited states estimated from finite chain calculations are too high because of chain end effects. Such errors are particularly large for double excitations, and this forces us to do an approximate calculation in the space of 0, 1, and 2 excitations from the single-particle picture for a relatively long chain, as opposed to an exact calculation for shorter chains. It is emphasized that energies of two-photon states calculated within this approach correspond to an upper limit [16]. In Fig. 3(b) we have plotted the absorptions from the $1B_u$ to the higher excited A_g states. In spite of the finite size effect that raises the energy of the biexciton, strong absorption to a biexciton state (labeled BX) below $2E(1^1B_u)$ is seen. We note in Figs. 3(a) and 3(b) that other optical transitions are available for the photogenerated $1B_u$ excitons. We expect therefore other PA bands to dominate the ir spectral range in the picosecond time domain. Recently such a PA band in the picosecond time domain has been detected [25]. From our theoretical calculations we expect the PA oscillator strength to be much larger in the ir spectral range ($1B_u \rightarrow mA_g$) than that in the visible range ($1B_u \rightarrow \mathrm{BX}$). The theoretical calculation gives a qualitative picture that complements the experimental work, based on which we suggest the energy-level diagram and the main optical transitions in PPV shown in Fig. 3(a).

We thank Val Masardier and D. Moses for providing us the PPV and PPV-MEH samples, respectively. The work at the University of Utah was supported in part by the DOE, Grant No. DE-FG-03-93, ER 45490 and by ONR Grant No. N00014-91-C-0104 at the Utah Laser Institute. At the University of Arizona, this work was supported by NSF, ECS-89-11960 and the AFOSR, Grant No. F49620-93-1-0199.

[1] S. N. Dixit, D. Guo, and S. Mazumdar, Phys. Rev. B **43**, 6781 (1991).
[2] Z. G. Soos, S. Etemad, D. S. Galvao, and S. Ramasesha, Chem. Phys. Lett. **194**, 341 (1992).
[3] Y. Kawabe *et al.*, Phys. Rev. B **44**, 6530 (1991).
[4] S. Abe, M. Schrieber, W. P. Su, and J. Yu, Phys. Rev. B **45**, 9432 (1992).
[5] Z. G. Soos *et al.*, Synth. Met. **54**, 35 (1993).
[6] J. H. Burroughes *et al.*, Nature (London) **347**, 539 (1990).
[7] R. Kersting *et al.*, Phys. Rev. Lett. **70**, 3820 (1993).
[8] U. Rauscher, H. Bässler, D. D. C. Bradley, and M. Hennecke, Phys. Rev. B **42**, 9830 (1990).
[9] C. J. Baker, O. M. Gelsen, and D. D. C. Bradley, Chem. Phys. Lett. **201**, 127 (1993).
[10] N. F. Colaneri *et al.*, Phys. Rev. B **42**, 11670 (1990).
[11] X. Wei, B. C. Hess, Z. V. Vardeny, and F. Wudl, Phys. Rev. Lett. **68**, 666 (1992).
[12] L. S. Swanson *et al.*, Phys. Rev. B **46**, 15072 (1992).
[13] J. Orenstein and M. Kastner, Solid State Commun. **40**, 85 (1981).
[14] U. Lemmer *et al.*, Appl. Phys. Lett. **62**, 2827 (1993).
[15] H. T. Grahn, Z. V. Vardeny, J. Tauc, and B. Abeles, Phys. Rev. Lett. **59**, 1144 (1987).
[16] P. Tavan and K. Schulten, Phys. Rev. B **36**, 4337 (1987).
[17] R. H. Austin, G. L. Baker, S. Etemad, and R. Thompson, J. Chem. Phys. **90**, 6642 (1989).
[18] D. Guo *et al.*, Phys. Rev. B **48**, 1433 (1993).
[19] The $1B_u$ and probably also the mA_g excitons in PPV-MEH are redshifted from those in PPV by 0.2 eV; L. Smilowitz and A. J. Heeger, Synth. Met. **48**, 193 (1992), and references therein. We also measured EA spectra of other PPV derivatives, such as PPV-DOD, with similar results.
[20] O. M. Gelsen *et al.*, Mol. Cryst. Liquid Cryst. **216**, 117 (1992).
[21] L. Sebastian and G. Weiser, Phys. Rev. Lett. **46**, 1156 (1981).
[22] G. Weiser, Phys. Rev. B **45**, 14067 (1992).
[23] P. Gomes da Costa and E. M. Conwell, Phys. Rev. B **48**, 1993 (1993).
[24] O. Akimoto and E. Hanamura, Solid State Commun. **10**, 253 (1972); W. F. Brinkman, T. M. Rice, and B. Bell, Phys. Rev. B **8**, 1570 (1973).
[25] L. Rothberg and M. Yan, in "Relaxations in Polymers," edited by T. Kobayashi (World Scientific, Singapore, to be published).